Design and Verification for Dual-mode CDFS and High-Load Compressor with a Large Flow Regulation Range

HUANG Lei[1,2], *ZHANG Jun*[2], *HAO Yuyang*[2], *REN Hongkai*[1], *CHU Wuli*[1*]

1. School of Power and Energy, Northwestern Polytechnical University, Xi'an 710072, P. R. China;
2. AECC Sichuan Gas Turbine Establishment, Chengdu 610500, P. R. China

(Received 11 May 2024; revised 18 July 2024; accepted 28 September 2024)

Abstract: This paper presents the design and verification of the dual-mode core driven fan stage (CDFS) and high-load compressor with a large flow regulation range. In view of the characteristics of large flow regulation range of the two modes and high average stage load coefficient, this paper investigates the design technology of the dual-mode high-efficiency compressor with a large flow regulation range and high-load compressor with an average stage load coefficient of 0.504. Building upon this research, the design of the dual-mode CDFS and four-stage compressor is completed, and three-dimensional numerical simulation of the two modes is carried out. Finally, performance experiment is conducted to verify the result of three-dimensional numerical simulation. The experiment results show that the compressor performance is improved for the whole working conditions by using the new design method, which realizes the complete fusion design of the CDFS and high-pressure compressor (HPC). The matching mechanism of stage characteristics of single and double bypass modes and the variation rule of different adjustment angles on performance are studied comprehensively. Furthermore, it effectively reduces the length and weight of compressor, and breaks through the key technologies such as high-load compressor with the average load factor of 0.504. These findings provide valuable data and a methodological foundation for the development of the next generation aeroengine.

Key words: fusion design; dual-mode; high-load compressor; large flow regulation range

CLC number: V231 **Document code:** A **Article ID:** 1005-1120(2024)05-0632-13

0 Introduction

The next generation aeroengine realizes the mode transition between the turbojet and turbofan working modes by changing the bypass ratio, so as to achieve the optimal performance in the flight envelope. During accelerating and supersonic flight processes, the engine works close to the turbojet mode with lower bypass ratio to increase the thrust. For the subsonic flight process, the engine operates as turbofan mode with higher bypass ratio to reduce fuel consumption and noise. The engine working mode transition not only requires a wide regulation range of bypass ratio at fan outlet, but also a variable bypass ratio for core engine. The core driven fan stage (CDFS) plays an important role in the engine bypass ratio regulation through the transition between the single and double bypass working modes[1-5], as shown in Fig.1. The single bypass working mode is that the first bypass duct is closed and the second one is open, and all the air from the fan flows through the CDFS. Then, part of the air flows out from the second bypass duct, and the rest goes into the high-pressure compressor (HPC). In the double bypass working mode, both the first and second bypass ducts are open, and part of the air from the fan enters the first bypass duct, and the other part flows through the CDFS. Then, the air flow downstream CDFS is further separated two

*Corresponding author, E-mail address: wlchu@nwpu.edu.cn.

How to cite this article: HUANG Lei, ZHANG Jun, HAO Yuyang, et al. Design and verification for dual-mode CDFS and high-load compressor with a large flow regulation range[J]. Transactions of Nanjing University of Aeronautics and Astronautics, 2024, 41(5): 632-644.

http://dx.doi.org/10.16356/j.1005-1120.2024.05.008

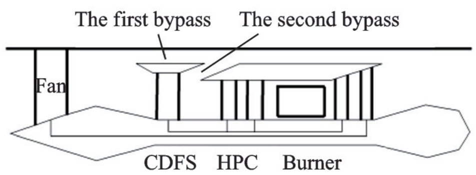

Fig.1 Schematic diagram of CDFS

parts. One flows out from the second bypass duct and mixes with the flow in the first bypass duct, and the other one goes into HPC.

The current generation of military turbofan engines with a high thrust-to-weight ratio has been developed and in service with a large number. For the compression component, the average stage pressure ratio is increased from 1.2 of the last generation engine to 1.3—1.4 of the current one. Therefore, the performance of the next generation engine has been greatly improved compared with the current turbojet and turbofan engines[6-8]. On the one hand, it is the technical difficulty of the next generation engine itself, such as the requirement for compression components to have a large flow regulation range and high efficiency while balancing high unit thrust and low fuel consumption modes, which is difficult for compression components to achieve. On the other hand, the compression component load is significantly increased[9], which requires HPC to achieve a higher total pressure ratio with fewer stages than the current engine. It has become one of the most important and difficult aspects for the next generation engine design.

The CDFS and compressor, as the core compression components of the next generation engine, have been conducted a lot of studies and experiments[10-13]. The GE21 demonstrator is the first application of CDFS in aeroengine. On this basis, general electric further develops the YF120, a current generation engine with a thrust-to-weight ratio of 10, and successfully conducts flight tests on the demonstration aircraft of the advanced tactical fighter. The CDFS in GE21 and YF120 are equipped with staters, and the guide vane of HPC is canceled. It adjusts the flow rate of HPC for different working states by using the CDFS staters, which can shorten the compressor length and reduce the blade number and weight, simultaneously improve the reliability. However, the disadvantage of this scheme is that the stage load is relatively low.

Zhang et al.[14-16] conducted the aerodynamic design of the CDFS and summarized the characteristics and difficulties. Specifically, they pointed out the importance of the shock loss control in the rotor design through analyzing the matching characteristics of the CDFS. Lai et al.[17] and Cao et al.[18] conducted optimization design of the CDFS, but it did not carry out relevant experimental verification. Zhou et al.[19] analyzed the influence of different inlet guide vane forms on the performance of the CDFS, but did not do related research and verification on the CDFS and compressor system design. Zhang et al.[20] and Liu et al.[21] studied the increasing stability margin of subsonic and transonic compressors, which revealed the internal flow mechanism of different structures. Wang et al.[22] analyzed the changes in the impact of different blade viscosities on compressor performance. Ma et al.[23] focused on the experiments design and verification for the external duct exhaust system of the CDFS and compressor matching. Huang et al.[24-25] performed a lot of work on CDFS and four-stage compressor for the next-generation engine. For the CDFS, a single-stage fan with high tangent velocity and low pressure ratio, has been designed, optimized and tested combined simulations and experiments. On this basis, the matching experimental test of the single-mode CDFS and compressor is conducted. In the matching experiments, the CDFS and compressor are designed separately and then verified in tandem. The separated design results in the CDFS with stator row and the HPC with guide vane, leading to the increase of length and weight of compression components. Most of studies are focused on the single-mode CDFS design and operating characteristics. There are some reports about the fusion design and verification of the CDFS and high-load compressors, but relatively few research on the high-load compressor combined with the dual-mode CDFS.

The present study performs a new integrated design method for a high-load four-stage compressor combined with a dual-mode CDFS fusion design, and conducts numerical and experimental verifications, laying a technical foundation for the development of the next generation engine.

1 Analysis of Difficulties in Dual-mode CDFS and High-Load Compressor Design

The reducing compressor stages and increasing stage load with much larger flow rate regulation range are always the development trend of the core compression components for the next generation engine. The most concerned challenges in the dual-mode CDFS and high-load compressor design include following two aspects.

(1) When the CDFS and the HPC transits from single bypass working mode to double bypass working mode, it is required that the reduction of rotation speed is less than 7%. The pressure ratio and efficiency should be almost kept unchanged, and the flow rate regulation range should reach more than 30%. For the conventional fan or compressor, the flow rate could only change about 15% with the rotation speed decrease of 7%. Combined with the guide vane regulation, it could realize more than 30%. But it would result in a large decrease in pressure ratio and efficiency. Therefore, it is a challenging work to balance the wide flow rate regulation range and high efficiency for the two modes.

(2) For the HPC, it requires that the compressor stages and rotation speed are as low as possible. The low rotation speed helps reduce the AN^2 value of the turbine and make the engine more realizable. But it prevents the compressor to achieve higher pressure ratio due to the reduction of the compressor rotor tip tangent speed. As a result, the average load coefficient of the compressor is significantly increased and reaches more than 0.5.

2 Pneumatic Design Results and Discussion

This section is focus on the two previous discussed challenges in the dual-mode CDFS and high-load compressor design. It presents the pneumatic design and verified results based on the integrated design method.

2.1 Design and research of high efficiency dual-mode CDFS and HPC with large flow regulation range

The balance between the two working modes should be taken into account in the parameter selection of design point for the dual-mode HPC. The single bypass working mode at 100% speed is chosen as the main design point with consideration of the double bypass mode working point. The dual-mode "1+4" scheme consists of a total of five stages of compressors. For the sake of consistency in description, the CDFS blade rows are defined as S0, R1, and S1, with stage number Stage 1. The blade rows of the high-pressure compressor are R2, S2, R3, S3, ⋯, R5, S5, with stage numbers Stage 2, Stage 3, ⋯, Stage 5, which will not be further explained later.

Taking into account the efficiency and surge margin of the two working modes of the scheme, the pressure ratio at design point is increased. In addition to the CDFS's certain requirement, the pressure ratio distribution of HPC stages is gradually reduced according to the characteristics of the tangential velocity reduction of the compressor from front to back. The distribution of pressure ratio is shown in Fig.2.

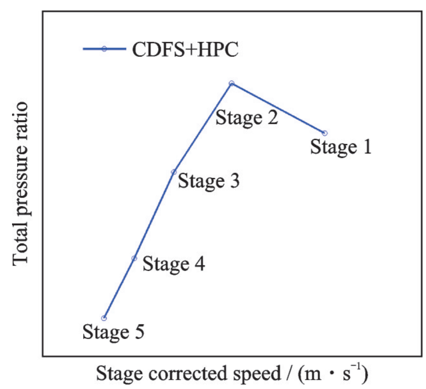

Fig.2 Schematic diagram for pulse generation and the experimental results

The working points matched at the rotor and stator of all stages are different for the two working modes. Some angles of attack of the rotor and stator in single bypass working mode are positive, and some of the row are negative. But the angle of attack of rotor and stator in double bypass working mode is changed. The angle of attack for rotor gradually decreases from the inlet stage to the rear stage as shown in Fig.3. The rotor blades at exit are opened a little to alleviate the blockage problem appeared at low rotation speed. The angle of attack for stator is selected as a relatively large value because of the negative value presented by the CDFS stator in dual-mode.

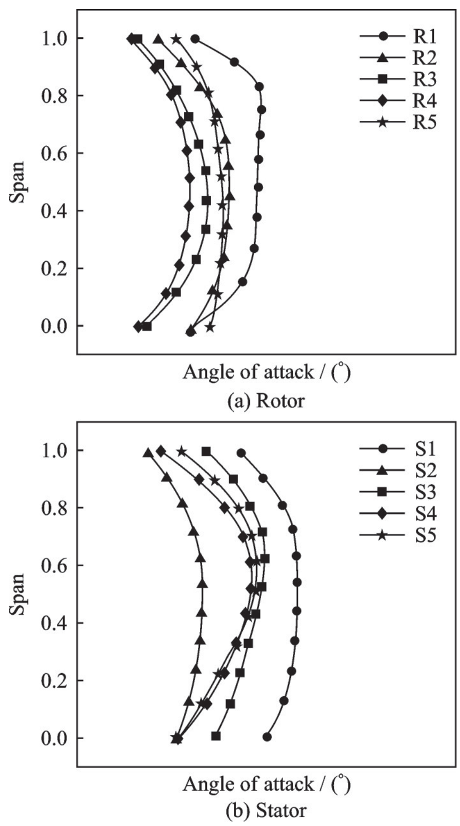

Fig.3 Angle of attack distribution

The matching analysis at design point for the stage characteristics is performed based on the one-dimensional middle diameter method and three-dimensional simulations. Fig.4 presents the stage pressure ratio distribution of all stages in different working modes. 1D represents the one-dimensional predicted characteristics and 3D the three-dimensional calculated characteristics. It is found that the stage pressure ratio distributions at the single bypass mode obtained by different methods agree well with the S2 flow design value at the 100% rotation speed. At the double bypass mode, the flow rate into the core engine decreases due to the opening of the first bypass duct. In order to adapt to the decrease in flow rate, the CDFS and compressor close the angle of the first two stages of guide vanes, causing a decrease in the pressure ratio of the first two stages. The pressure ratio of the last three stages is closer to the design value of the S2 flow surface, thus achieving a wide range of flow regulation.

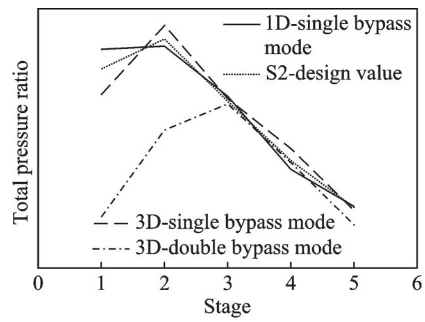

Fig.4 Stage pressure ratio distribution of different working modes

The stage matching characteristics of the “1+4” scheme are analyzed at the conditions from chock to near surge based on the three-dimensional simulations. The results in Fig.5 show that the predicted stage matching characteristics agree well with the S2 flow design value and work at the high efficiency area for both two working modes. For the single bypass mode at 100% rotation speed, all stages work adequately well and keep high efficiency. For the double bypass mode at working rotation speed, the pressure ratios of the first two stages are declined markedly by 16%—20% due to the guide vane angle decrease. The pressure ratio of rear three stages is decreased slightly. It is because that the rotation speed at the double bypass mode is lower than that at the single bypass mode.

The current scheme realizes a large flow rate regulation combined rotation speed reduction and guide vane angle variation. In this scheme, the two modes of the compressor have a slip of about 7% and the efficiency remains basically unchanged. However, the flow regulation range needs to reach more than 30%. In order to achieve a wide range of flow regulation, it is necessary to adjust the guide vanes at a large angle, which will inevitably cause a sharp increase in the loss of the guide vanes when they deviate significantly from the design angle. According to the requirements of low loss adjustment in large flow range, the design of adjustable guide

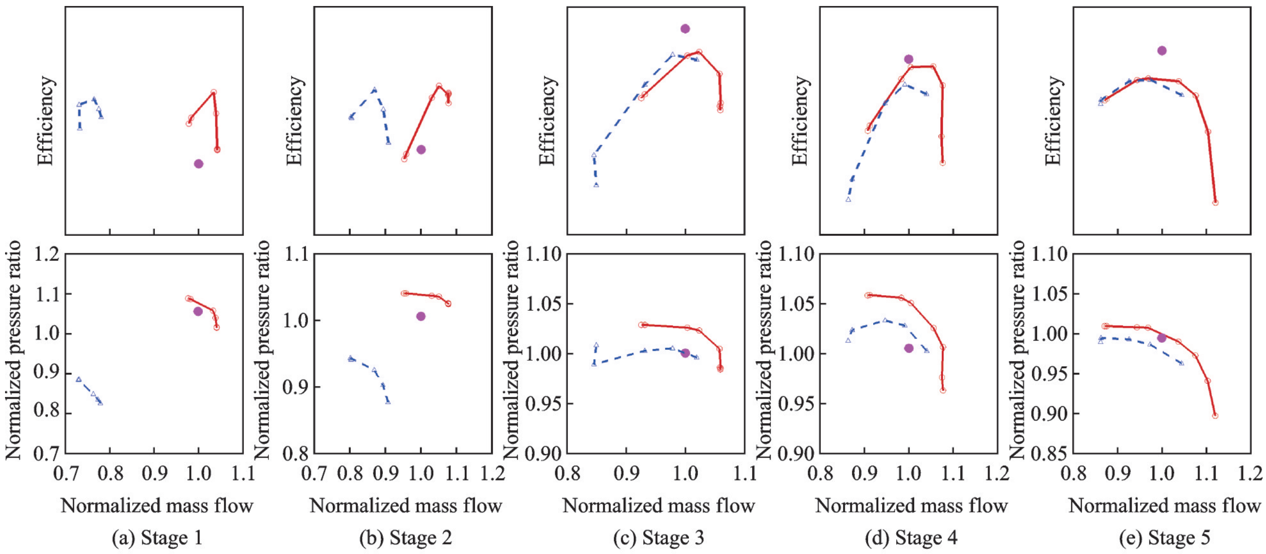

Fig.5 Predicted stage matching characteristics for two working modes

vane with low loss is studied. After research, it is found that the front section of the variable camber guide vane is fixed and the back section is adjustable, which solves the large separation of suction surface caused by large closing angle of conventional guide vane and has the characteristic of low loss adjustment. As shown in Fig.6, it presents the total pressure recovery coefficient for two different guide vane designs at the same flow condition. It is found that the loss of the variable camber guide vane is greatly reduced. Therefore, the variable camber guide vane design with low flow loss plays an important role in the current scheme for its high working efficiency. The effects of the gap structures and multi-parameter selection on the variable camber guide vane performance are further discussed.

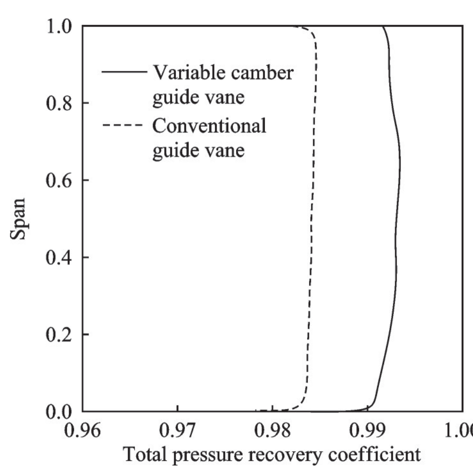

Fig.6 Comparison of total pressure recovery coefficient between variable camber guide vane and conventional guide vane

The gap structure between the front and back segments of the variable camber guide vane not only affects the blade loss, but also determines the intensity of the secondary flow from pressure surface to the suction surface. Therefore, three different gap structures without gap, cuneate gap and circular gap are compared and analyzed. Both the gap width is 0.05 mm. The predicted aerodynamic loss of the three guide vane structures by simulations are shown in Fig.7. The analysis results indicate that the presence of guide vane gaps leads to a secondary flow of airflow with a certain intensity towards the suction side, inducing thickening of the surface boundary layer on the suction side and accompanied by a certain degree of separation flow phenomenon.

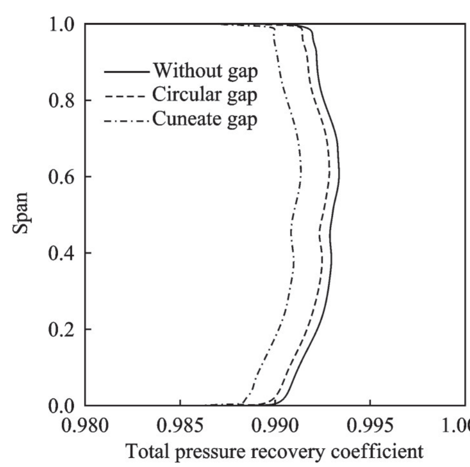

Fig.7 Total pressure recovery coefficient comparison between three gap structures

As shown in Fig.7, it increases the flow loss and mixing loss and leads to a reduction of the total pressure recovery coefficient. Compared with the gap structure, the circular structure weakens the secondary flow intensity and suppresses the separation zone, which makes the total pressure restore nearly to the without gap level.

The parameters, such as the maximum thickness of blade and its location, the position of the deflection axis, play dominant role in the aerodynamic loss control of the variable camber guide vane. The maximum thickness is generally determined by the strength requirement. Generally, the aerodynamic loss becomes smaller when the position of blade maximum thickness is closer to the rear, while it is opposite for the deflection axis with the position closer to the front. However, the couple effect of these two factors on the variable camber guide vane still need be further studied.

Therefore, the computational fluid dynamics (CFD) methods are used to calculate, analyze, and screen multiple samples at different thickness positions and different offset axis positions. After comprehensive consideration of multiple performance indicators (aerodynamic loss, lag angle, flow deviation), the selection range of optimization design parameters is determined (as shown in Fig.8). The optimization scheme is obtained by using the multi-parameter performance optimization design method based on the optimization selection range of the design parameters. The simulation results show that the optimized scheme has less aerodynamic loss than the original scheme with the efficiency increased by about 0.2% as shown in Table 1.

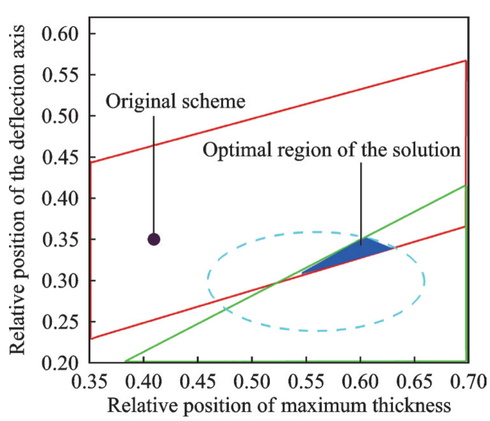

Fig.8 Optimization of design parameters

Table 1 Aerodynamic performance of optimization scheme

Scheme	Total pressure recovery coefficient	Efficiency
Original scheme	0.991 9	0.857 0
Optimization scheme	0.995 0	0.859 1

2.2 Design technology of high-load HPC with average load coefficient of 0.504

The average load coefficient of the compressor is the arithmetic average value of every stage load coefficient. The stage load coefficient is calculated by using the ratio of the flange work to the square of tangential velocity in the middle blade height.

$$H_T = \frac{\Delta h}{U_m^2} = \frac{C_P \Delta T}{U_m^2} \tag{1}$$

where H_T is the stage load coefficient of the compressor, U_m the rotor tangential velocity at the middle blade height, Δh the enthalpy increase of the compressor stage, C_P the specific heat of the gas at constant pressure, and ΔT the temperature rise of the compressor stage.

The design parameter selection for the high-load compressor is quite different from that of the conventional one. It is focused on the load design of the rotor and stator, meridional flow path design and high-load blade design.

It is important to carry out load redistribution design between the rotor and stator with the given stage load. The most critical parameter to control the rotor and stator load is the pre-whirl of the stator, which directly affects the stage reaction degree. The rotor load is aggravated and it becomes more difficult for air decelerating and diffusing in the rotor blade with the increase of the reaction degree valve. Conversely, the stator load is increased with the decrease of the reaction degree valve. As shown in Fig.9, the stage reaction degree distribution of the current high-load scheme is 0.8%—11.5% higher than the conventional load one. Because the stator is more prone to separation and stall in the high-load compressor. Therefore, the higher reaction degree value is selected to increase the rotor load and allevi-

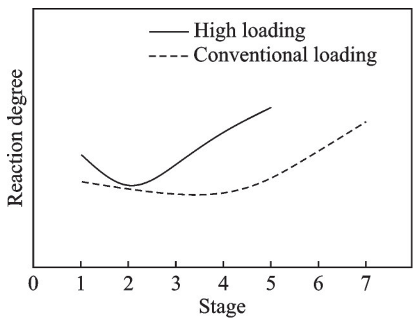

Fig.9 Stage reaction degree distribution of high-load and conventional load compressors

ate the stator load. The design helps to improve the margin of high-load compressor while taking into account the efficiency.

The diffusion factors (D-factor) of the rotor and stator for the current high-load scheme are also much larger than the conventional load one as shown in Fig.10. It can be seen that the rotor load is heavier. The root and tip of the rotor blade exceeds 0.5 and keeps relatively appropriate within the acceptable range for the stator blade. The diffusion factor of the conventional compressor rotor is generally about 0.4, and the stator is generally about 0.43, which is far lower than the current scheme.

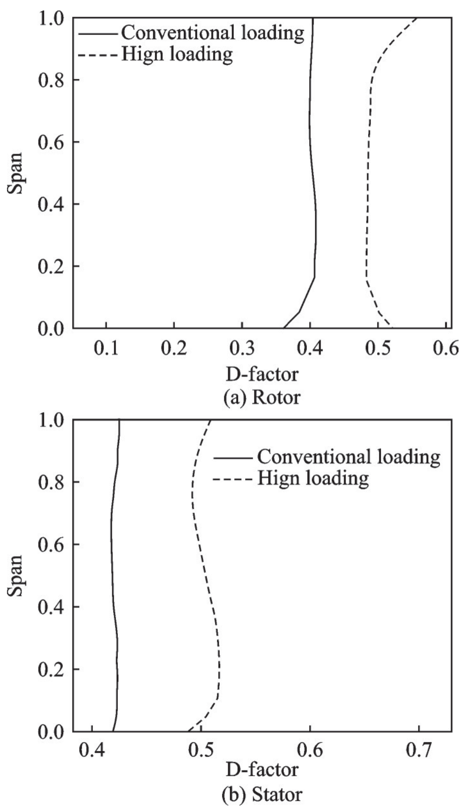

Fig.10 Diffusion factor distribution of high-load and conventional load compressors

The inner meridional flow path of the high-load compressor adopts a certain curvature design in each blade row. The outlet of the flow path is raised for the part of the rotor, and the corresponding inlet height of the next blade row is reduced as shown in Fig.11. It makes for the increasement of the Dehaller number and the axial density flow velocity ratio (AVDR) of the rotor and stator. It can effectively reduce the inlet Mach number of the stator, and make the compressor more stable with higher efficiency and wider stability margin. In addition, the blade adopts a compound sweep shape, and the rotor adopts a forward-sweep design, improving the aerodynamic performance and suppressing the blade vibration.

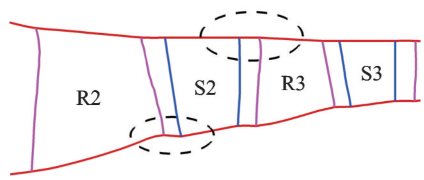

Fig.11 Meridional flow path projection of local scheme

The blade profile design mainly focuses on the effects of aspect ratio, consistency and curved-sweep on the high load characteristics of the current dual-mode “1+4” scheme. The selection of molding parameters of the rotor and stator at all levels takes into account the design of both modes.

Blade aspect ratio has an important effect on the compressor performance and stable working range. According to the previous experience, when the aspect ratio is smaller than 0.5, the compressor efficiency reduces with the aspect ratio decrease due to the severe radial mixing. When the aspect ratio is larger than 3, the efficiency also reduces with the increase of aspect ratio. It is because that the turning angle of air flow per unit length is increased on the narrow blade, leading to a serious separation and the increase of flow loss. In addition, the surge margin of the compressor decreases with the increase of aspect ratio. The requirement for stall margin is also increased in the high-load compressor design. As a result, the aspect ratio is developing to a smaller value. It helps to reduce the inverse pressure gradient on the blade surface and boundary layer growth rate on the endwall with the large blade chord length design.

Consistency is the ratio of blade chord length to cascade spacing. In the high-load compressor design, the blades are designed with large turning angle to achieve more work added to the air flow. The control ability of air flow and the stall margin is increased with consistency under a certain aspect ratio. However, the higher consistency brings more flow loss due to the wall friction, leading to the efficiency decrease. Therefore, it is necessary to choose the consistency of the rotor and stator reasonably. With the increase of compressor load, the consistency is developing towards a larger direction, known as large consistency design.

Blade sweep technology is a new type of three-dimensional aerodynamic layout design. The three-dimensional structure of the shock wave at compressor inlet is reorganized through the blade meridional sweep design. It helps to reduce the normal component of the relative Mach number at the rotor tip, leading to the shock loss and its interaction with boundary layer weakened and the compressor efficiency and margin improved. The curved stator blade also helps to improve the compressor efficiency and margin by eliminating or delaying the flow separation in the corner region.

The rotor blades of R1—R4 are swept and stators of S3—S5 are curved in current high-load scheme as shown in Fig.12. It improves the three-dimensional flow inside the compressor, thereby reducing the strong secondary flow inside the channel, improving the efficiency and stable working margin of the compressor. The curved stator is bent of middle of the blade height towards the pressure surface.

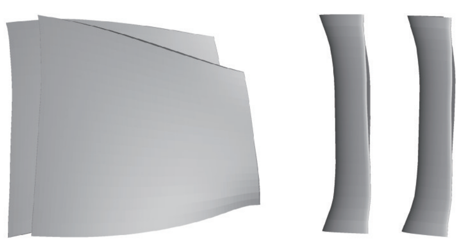

Fig.12 Forward-swept rotor and curved stator

3 Dual-mode CDFS and Compressor Performance Evaluation

The impact of different operating conditions on CDFS and compressor performance is evaluated by three-dimensional steady simulations with NUMECA software. The Reynolds averaged Navier-Stokes equations combined with Spalart-Allmaras turbulence model are solved with central difference scheme with the second order accuracy in the calculation process. The absolute total temperature, total pressure and flow angle are specified at the inlet. The different average static pressures are set at the outlet to obtain the working characteristics, and the bleed rate of the second bypass duct is given according to the fixed proportion of CDFS inlet flow (a fixed bypass ratio).

Firstly, grid independence validation is conducted on three different grid scales with $Y+$ less than 10 at the wall, labeled as grid 1 with 2.6 million cell nodes, grid 2 with 3.42 million cell nodes, and grid 3 with 4.8 million cell nodes, respectively. After calculation and analysis, the calculation results of the 4.8 million grid are very close to those of the 3.42 million grid. Considering the calculation period, the results calculated using the 3.42 million unit nodes in grid 2 are reliable. Except for the grid scale that has been verified for grid independence, all other calculation settings have been validated using compressors with similar loads in the past to ensure the accuracy of three-dimensional steady-state simulation.

Then, the flow characteristics of the working point under the single and double bypass modes are compared and analyzed. It is found that there is no obvious flow separation on the surface of each blade row near the operating point at the 100% rotation speed for single bypass mode as shown in Fig.13(a). The shock waves appear at the rotor tip for the first three stages because of supersonic. The shock waves in the first stage consist of an oblique shock and a normal shock, and there is no large separation downstream the shocks or in the stator channel. It proves that the load distribution is reasonable. There is also no obvious flow separation on the surface of each blade row near the working point at the 92.4% rotation speed for double bypass mode as shown in Fig.13(b). However, the first stator closing angle is large according to the mass flow rate adjustment requirement. It leads to a negative attack angle of the blade. In addition, the pressure ratio of the first two stages decreases due to closing the adjustable guide vane angle of the first two stages, combined with low rotor speed front stage surge and rear stage blockage characteristics. It can make all levels of the blade better match in its low loss angle of attack range. In general, the flow field distribution is reasonable, which ensures the efficiency and stability margin of the dual-mode "1+4" scheme.

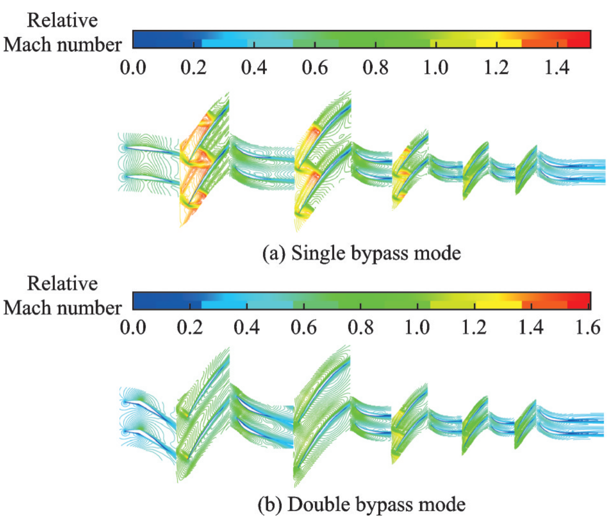

(a) Single bypass mode

(b) Double bypass mode

Fig.13 Relative Mach number distribution at 90% blade height section for different working modes

Based on the analysis of the flow field, in order to study the effect of different regulation rules on the performance of the dual-mode "1+4" scheme, the characteristics of the CDFS and compressor at different rotating speeds are calculated by the full three-dimensional NUMECA software. The design angle, the opening angle and the closing angle are calculated, respectively.

Fig.14 shows a comparison of the characteristics of different regulation rules. The set of rules for relative conversion speeds of 0.9, 0.85, and 0.8 degrees of closing angle is based on the design rules, with S0 closing 13 degrees more and S1 closing 6.5 degrees more. The set of rules for opening angle mainly includes S0 opening 5 degrees more and S1 opening 2.5 degrees more at speeds of 0.95 and below. It can be seen that when the large angle is closed, the total flow and the maximum efficiency is reduced, and the boundary is widened. When the angle is opened, the total flow is increased. The maximum efficiency is almost the same as that of the design angle and the boundary is slightly reduced.

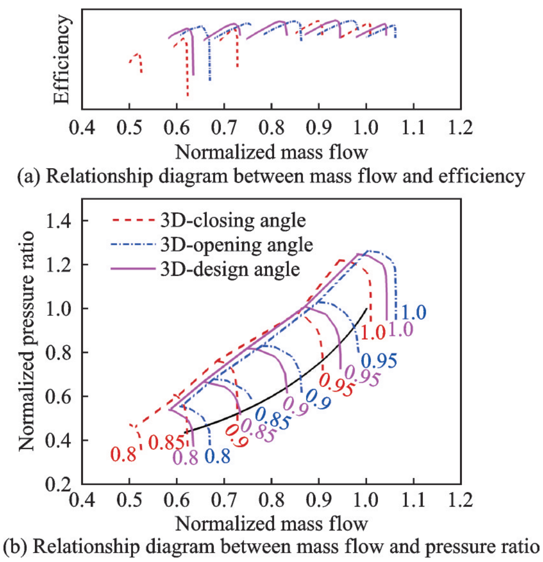

(a) Relationship diagram between mass flow and efficiency

(b) Relationship diagram between mass flow and pressure ratio

Fig.14 Comparison of characteristics with different regulation rules

The variation law of different adjustment angles on performance provides optimization direction for the engine performance, and provides data support for the formulation of control laws. The following test results are consistent with the trend of numerical simulation, proving that the matching design of CDFS and HPC and the numerical simulation method are correct.

4 Experimental Verification

The experimental verifications of the dual-mode CDFS and the high-load four-stage compressor scheme are conducted by a compressor test bench. Electronic pressure scanning valve, data collection system and dynamic collection system are used in the test. Before the test, the measurement and calibration of the test system are carried out. After precision analysis, the measuring accuracy of the total pressure is ±0.2%, and the measuring accuracy of the total temperature is ±0.6%, which meets the test requirements.

In the test scheme, in addition to the conventional total performance parameters such as the flow rate total temperature and the total pressure at the inlet and outlet. In specifically, 9-point sensors are set along the radial direction at the leading edge of S1 respectively to obtain the total temperature and pressure at the outlet of the CDFS rotor, respectively. 5-point sensors are installed along the radial direction at the leading edge of S2—S5 respectively, which are used to measure the total temperature and pressure at the rotor outlet for each stage of HPC, respectively. During the experiments, the outlet reverse pressure is controlled by the opening of the exhaust throttle to obtain the characteristic line, and the required bypass ratio is ensured by adjusting the air flow of the second bypass. For CDFS and high load four stage compressor component tests, the method of switching between single and double bypass modes mainly relies on the differences in speed, guide vane adjustment angle, and the bypass ratio of the second bypass to achieve the switching between the two modes. The single bypass mode has corresponding speed, guide vane adjustment angle and bypass ratio. The double bypass mode is also the same.

4.1 Total characteristic analysis

The total performance and surge boundary of the high-load compressor are obtained in the experiments at the relative conversion speed 80%—100% for single bypass mode and at the relative conversion speed 92.4% for double bypass mode as shown in Fig.15. The results show that the experimental characteristics are in good agreement with the 1D, and the 3D is basically in agreement with the experimental data, except that the calculated flow rate is 2% larger than the measured value. It conforms to the usual design rules. It is confirmed the accuracy of the 1D and 3D simulation methods for current dual-mode "1+4" scheme prediction.

The experimental results show good performance in all considered conditions for both working modes. The highest efficiency reaches 0.874 at the relative conversion speed 100% for single bypass mode. The highest efficiency reaches 0.870 at the relative conversion speed 92.4% for double bypass mode. The adjustment range of the flow rate reaches 31.4% with high efficiency and wide stable margin. In the full speed range considered, the highest efficiency reaches 0.89 at the relative conversion speed 90%. The whole efficiency envelope is good. The stable margin at every working rotation speed line is not less than 25%. There are no obvious pits on the boundary and the match of all stages is balanced. Thus the pressure ratio of the seven-stage compressor of the current generation engine is realized by using the five-stage compressor. The average load coefficient is increased by 40%, which is much higher than the compressor load level of the F119 engine.

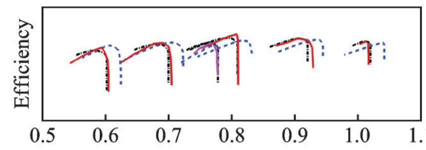

(a) Relationship diagram between mass flow and efficiency

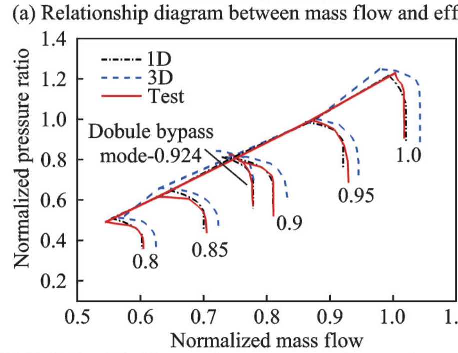

(b) Relationship diagram between mass flow and pressure ratio

Fig.15 Comparison of total performance test characteristics and design characteristics

4.2 Stage characteristics analysis

In order to further analyze the matching status of each stage, the working status of each stage under the two modes is analyzed according to the total temperature and pressure measured by the experiment. Fig.16 shows the comparison between the test characteristics of each stage at the relative conversion speed 100% and the three-dimensional calculation in the single bypass mode. As can be seen from the figure, the pressure ratio at all stages reaches the S2 design value, and the efficiency at all stages basically reaches the S2 design value, which is in line with the design expectation. The stage characteristics of the test and three-dimensional calculations are basically consistent, indicating that the pressurization capacity at all stages meets the design expectations. The pressure ratio at all stages gradually increases with the decrease of flow rate, and there is no stage with the lower pressure ratio, indicating that the characteristics of all stages are well matched. The second stage has a high efficiency due to the high pressure ratio of the stage, and the other stages are basically matched in the high efficiency zone. In addition, the efficiency of the third stage decreases firstly with the increase of pressure ratio, which can be judged to be the priority occurrence stage of stall. In general, it can be seen that each stage is basically matched in its own working point and high efficiency zone, and the overall match is still relatively good.

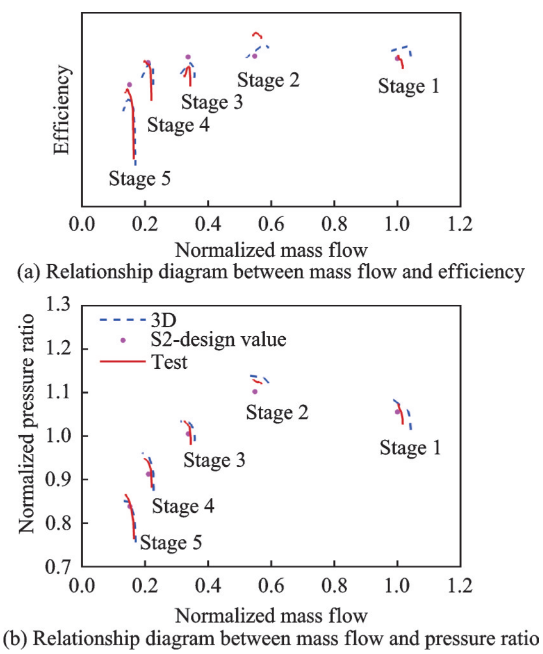

(a) Relationship diagram between mass flow and efficiency

(b) Relationship diagram between mass flow and pressure ratio

Fig.16 Stage characteristics and simulation results for single bypass mode

Fig.17 shows the comparison between the measured stage characteristics at the relative conversion speed 92.4% for double bypass mode and the simulation results. It can be seen from the figure that the trend of test and three-dimensional calculation characteristics is basically the same. With the decrease of the flow rate, the pressure ratio of the third stage increases first and then decreases, while the pressure ratio of the other stages does not decrease, indicating that the third stage for double bypass mode can be judged to be the priority occurrence stage of stall, thereby inducing surge. In general, it can be seen that each stage is basically matched in its own working point and high efficiency zone, and the overall match is still relatively good.

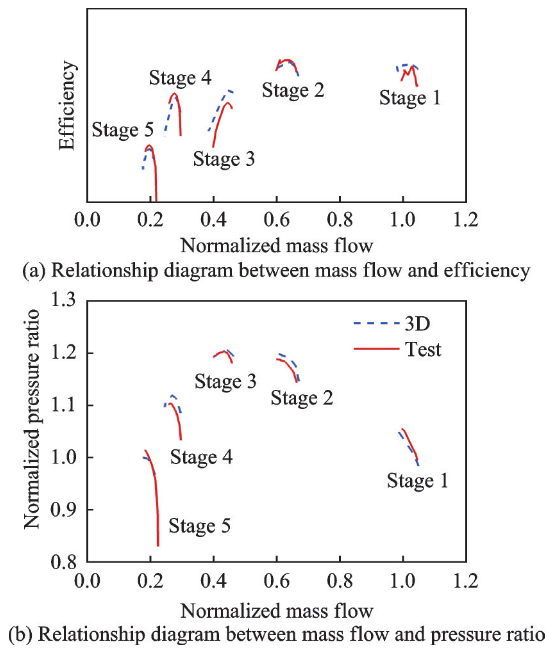

(a) Relationship diagram between mass flow and efficiency

(b) Relationship diagram between mass flow and pressure ratio

Fig.17 Stage characteristics and simulation results for double bypass mode

5 Conclusions

This study focuses on the design and verification of the high-load four-stage compressor combined with a dual-mode CDFS through simulations and experiments. Significantly, it makes a breakthrough in high-load compressor with the average load factor of 0.504 and the dual-mode high-efficiency compressor with a large flow regulation range of 31.4%. The results provide valuable data and methodological support for the development of the next generation aeroengines. Based on the study of dual-mode "1+4" scheme and the experimental verifications, the following conclusions can be drawn as follows:

(1) For dual-mode CDFS and HPC, load distribution and angle of attack selection should be done well in the initial design to balance the two modes, which should make the two components match at the best working point as far as possible.

(2) The variable camber guide vane with the

circular gap structure designed by multi-parameter performance optimization method exhibits superior performance for the large flow rate range regulation.

(3) The performance of the compressor can be improved by using meridian projection composite sweep shape, appropriate pre-whirl of the stator, raising the flow channel at the root of the rotor outlet and lowering the flow channel at the inlet of the stator, as well as designing a small aspect ratio composite curved sweep rotor stator。

(4) The performance of the dual-mode "1+4" scheme can be effectively evaluated through the one-dimensional and three-dimensional simulations, which can provide effective technical support for engine test verification. The experimental results demonstrate that the flow regulation range of the two modes in the high efficiency range reaches 31.4%.

In conclusion, the test shows that the dual-mode CDFS and compressor exhibit excellent performance in all working conditions. The flow rate, pressure ratio and efficiency of the two modes with the single and double bypasses reach the design index, which verifies the validity of the design method of the dual-mode high-load compressor with a large flow regulation range. The development experience provides valuable technical support for the research of the next generation of the engine compressor.

References

[1] FANG C. Variable cycle engine and its key technologies[J]. Aviation International, 2004, 17(3): 1-5.

[2] LIN X. Research on steady state performance calculation of variable geometry engine[D]. Xi'an: Northwestern Polytechnical University, 2004.

[3] RALLABHANDI S K, MAVRIS D N. Simultaneous airframeand propulsion cycle optimization for supersonic aircraft design: AIAA—2008-143[R]. [S.l.]: AIAA, 2008.

[4] BROWN R. Integration of a variable cycle engine conceptin a supersonic cruise aircraft: AIAA—79-1049 [R]. [S.l.]: AIAA, 1979.

[5] FRENCH M W, ALLEN G L. NASA VCE test bed engine aerodynamic performance characteristics and test results: AIAA—81-1594[R]. [S.l.]: AIAA, 1981.

[6] VDOVIAK J W, KNOTT P R, EBACKER J J. Aerodynamic acoustic performance of YJ101 double bypass VCE with coannular plug nozzle: NASA-CR-159869[R]. [S.l.]: NASA, 1981.

[7] JOHNSON J E. Variable cycle engine developments at general electric: AIAA—97-15033[R]. [S.l.]: AIAA, 1997.

[8] ALLAN R D. General electric company variable cycle engine technology demonstrator programs: AIAA—79-1311[R]. [S.l.]: AIAA, 1979.

[9] LI Qinghua, AN Liping, XU Lin, et al. Design and test verification of high load axial-flow compressor[J]. Acta Aeronautica et Astronautica Sinica, 2017, 38 (9): 520990. (in Chinese)

[10] HOWLETTE R A, SABATELLA J, JOHNSON J, et al. Advanced supersonic propulsion study: NASA-CR-134904[R]. [S.l.]: NASA, 1975.

[11] NASCIMENTO M A R. The selective bleed variable cycle engine[D]. Bedfordshire, UK: Cranfield Institute of Technology, 1992.

[12] KNOTT P R, BRAUSCH J F, BHUTIANI P K, et al. VCE early acoustic test results of general electric's high-radius ratio coannular plug nozzle: NASA-CR-99076[R]. [S.l.]: NASA, 1980.

[13] STEVEN G, BERNARD L. Engine design and challenges for the high mach transpor: AIAA—2007-5334 [R]. [S.l.]: AIAA, 2007.

[14] ZHANG Xin, LIU Baojie. Analysis of aerodynamic design characteristics of fan stage driven by core engine[J]. Journal of Aerodynamics, 2010, 25(2): 434-442. (in Chinese)

[15] ZHANG X, LIU B. Influence analysis of fan stage design parameters of compact layout core engine[J]. Chinese Journal of Propulsion, 2011, 32(1): 47-58.

[16] ZHANG Xin, LIU Baojie. Matching characteristics of core driven fan stage[J]. Acta Aeronautica et Astronautica Sinica, 2015, 36(9): 2850-2858. (in Chinese)

[17] LAI A, HU J, TU B. Pneumatic design scheme of core engine driven fan stage[J]. Journal of Aerodynamics, 2014, 29(9): 2229-2238.

[18] CAO H, ZHOU Z, HU J, et al. Aerodynamic optimization design of fan level driven by core machine with both modes[J]. Journal of Aerodynamics, 2018, 33 (3): 717-728.

[19] ZHOU L, LIU D, WANG Z. Influence of inlet guide vanes type on core driven fan stage[J]. Journal of Aerospace Power, 2018, 33(7): 1676-1684.

[20] ZHANG H, ZHANG C, DONG F, et al. Effect of different radial inclined angles of self-circulation casing treatment on the transonic axial flow compressor performance[J]. Journal of Applied Fluid Mechanics, 2023, 16(3): 533-547.

[21] LIU H W, CHU W L, ZHANG H G, et al. Effect of inclination grooves on axial flow compressor stability: An experimental and numerical simulation study[J]. Journal of Applied Fluid Mechanics, 2023, 16(2): 311-323.

[22] WANG Tonghui, WANG Zhiqiang, WANG Xuegao. Numerical simulation of influence of blade number on maximum stall static pressure rise of compressor[J]. Journal of Nanjing University of Aeronautics & Astronautics, 2022, 54(4): 662-669.(in Chinese)

[23] MA C, HOU M, LIANG J, et al. Design and test verification of a core engine fan stage matching test with a high-pressure compressor[J]. Gas Turbine Test and Research, 2019, 33(1): 6-11.

[24] HUANG L, YU H. Multi-objective optimization design of rotor blades of single-stage transonic fan[J]. Gas Turbine Test and Research, 2016, 29(3): 30-34.

[25] HUANG L, ZHOU B, LI Q, et al. Design technology and test verification of high tangential velocity low pressure ratio single-stage fan[J]. Gas Turbine Test and Research, 2016, 29(6): 16-20.

Acknowledgement This work was supported by the National Major Project.

Authors Mr. **HUANG Lei** obtained the M.S. degree in engineering from Northwestern Polytechnical University in 2009, and entered Northwestern Polytechnical University to pursue a Ph.D. degree in Engineering in 2019. He currently works as a researcher at AECC Sichuan Gas Turbine Establishment. His main research area is the aerodynamic design of aircraft engine compressors.

Prof. **CHU Wuli** obtained the M. S. degree in engineering from Xi'an Jiaotong University in 1987, and obtained the Ph.D. degree in engineering from Northwestern Polytechnical University in 1999. He is a professor and doctoral supervisor at Northwestern Polytechnical University. His main research area is the stability and flow control technology of aviation turbomachinery.

Author contributions Mr. **HUANG Lei** designed the study, complied the models, conducted the analysis, interpreted the results and wrote the manuscript. Mr. **ZHANG Jun** contributed to data and model components. Mr. **HAO Yuyang** revised the article according to the reviewer's comments. Mr. **REN Hongkai** contributed to data for the analysis. Prof. **CHU Wuli** contributed to the discussion and background of the study. All authors commented on the manuscript draft and approved the submission.

Competing interests The authors declare no competing inrests.

(Production Editors: XU Chengting, WANG Jie)

大流量范围双模式CDFS和高负荷压气机设计研究与验证

黄 磊[1,2], 张 军[2], 郝玉扬[2], 任洪凯[1], 楚武利[1]

(1.西北工业大学动力与能源学院,西安710072,中国; 2.中国航发四川燃气涡轮研究院,成都610500,中国)

摘要:介绍了大流量范围双模式核心驱动风扇(Core driven fan stage, CDFS)和高负荷压气机的设计研究与验证。针对其两个模式流量变化范围大、平均级载荷系数高等特点,研究大流量调节范围双模式高效率压缩部件设计技术、平均载荷系数0.504的高负荷压缩部件设计等技术,并在此基础上完成双模式CDFS与四级压气机的设计,开展两种模式的三维流场分析,最终通过试验验证三维数值模拟的结果。试验结果表明:全新的一体化设计技术应用提高了全工况的性能,有效地使CDFS和高压压气机(High-pressure compressor, HPC)缩短了长度,减轻了重量,实现了两个部件的完全融合设计,全面研究了单外涵和双外涵模式的级特性匹配机理以及不同调节角度对性能的变化规律,突破了平均载荷系数0.504的高负荷压缩部件设计等关键技术,为下一代发动机的核心压缩部件设计奠定了基础。

关键词:融合设计;双模式;高负荷压气机;大流量范围